

Article

Investigating Tensile Behavior of Sustainable Basalt–Carbon, Basalt–Steel, and Basalt–Steel-Wire Hybrid Composite Bars

Mohammadamin Mirdarsoltany ^{1,*}, Alireza Rahai ¹, Farzad Hatami ¹, Reza Homayoonmehr ¹
and Farid Abed ²

¹ Department of Civil Engineering, Amirkabir University of Technology, Tehran 15875-4413, Iran; rahai@aut.ac.ir (A.R.); hatami@aut.ac.ir (F.H.); rhomayoonmehr@aut.ac.ir (R.H.)

² Department of Civil Engineering, American University of Sharjah, Sharjah 61125 79999, United Arab Emirates; fabled@aus.edu

* Correspondence: amin.st@aut.ac.ir

Abstract: One of the main disadvantages of steel bars is rebar corrosion, especially when they are exposed to aggressive environmental conditions such as marine environments. One of the suggested ways to solve this problem is to use composite bars. However, the use of these bars is ambiguous due to some weaknesses, such as low modulus of elasticity and linear behavior in the tensile tests. In this research, the effect of the hybridization process on mechanical behavior, including tensile strength, elastic modulus, and energy absorbed of composite bars, was evaluated. In addition, using basalt fibers because of their appropriate mechanical behavior, such as elastic modulus, tensile strength, durability, and high-temperature resistance, compared to glass fibers, as the main fibers in all types of composite hybrid bars, was investigated. A total of 12 hybrid composite bars were made in four different groups. Basalt and carbon T300 composite fibers, steel bars with a diameter of 6 mm, and steel wires with a diameter of 1.5 mm were used to fabricate hybrid composite bars, and vinyl ester 901 was used as the resin. The results show that, depending on composite fibers used for fabrication of hybrid composite bars, the modulus of elasticity and the tensile strength increased compared to glass-fiber-reinforced-polymer (GFRP) bars by 83% to 120% and 6% to 26%, respectively. Moreover, hybrid composite bars with basalt and steel wires witnessed higher absorbed energy compared to other types of hybrid composite bars.

Keywords: composite bars; hybrid composite bars; hybridization process; BFRP bars; GFRP bars



Citation: Mirdarsoltany, M.; Rahai, A.; Hatami, F.; Homayoonmehr, R.; Abed, F. Investigating Tensile Behavior of Sustainable Basalt–Carbon, Basalt–Steel, and Basalt–Steel-Wire Hybrid Composite Bars. *Sustainability* **2021**, *13*, 10735. <https://doi.org/10.3390/su131910735>

Academic Editors: Sebastian Kot and Mariusz Urbański

Received: 31 August 2021

Accepted: 22 September 2021

Published: 27 September 2021

Publisher's Note: MDPI stays neutral with regard to jurisdictional claims in published maps and institutional affiliations.



Copyright: © 2021 by the authors. Licensee MDPI, Basel, Switzerland. This article is an open access article distributed under the terms and conditions of the Creative Commons Attribution (CC BY) license (<https://creativecommons.org/licenses/by/4.0/>).

1. Introduction

Steel bars are some of the most widely used materials in the construction industry [1]. One of the drawbacks of steel bars is their low durability against aggressive environmental conditions, including marine environments and cities' atmospheres containing high CO₂ concentrations, which cause corrosion of these bars in reinforced-concrete (RC) elements [2–4] and therefore reduce the long-term performance of them [5–7]. It is worth mentioning that it is proposed that, regardless of the binder composition, a simultaneous carbonation and chloride attack increases the potential for corrosion of rebars [8]. Besides financial costs due to maintenance and repair of corroded reinforced-concrete (RC) structures, rebar corrosion can cause structural safety risks by reducing the cross-section of rebars, concrete cracking, and reducing the bonding of concrete and rebars [9–11]. Apart from corrosion of the steel bars, some factors, such as the embedded length of the bars in the concrete, threat strength, and loading rate, play a pivotal role in the load capacity of bars [11,12].

Researchers have proposed different ways to overcome steel-corrosion problems in RC elements, mainly divided into three methods. The first method is to use a hybrid system in such a way that steel and composite bars are used simultaneously in the reinforced-concrete section [1,13–15]. Despite the decrease in the percentage of steel reinforcement in

the cross-section of RC elements due to the presence of steel reinforcement, the corrosion problem is not entirely addressed.

The second method is to enhance the properties of concrete in such a way that it has less permeability. This method can be referred to as using additives to concrete such as pozzolans [16–21] or reducing the ratio of water to cement in the concrete mixing design [9,22,23].

The third method is the use of composite bars that can be an appropriate way to solve the problem of rebar corrosion [24,25]. These bars have acceptable properties, such as environmental durability and acceptable resistance to corrosion [6,25–33]. However, the use of this method is limited due to the low modulus of elasticity of these bars [32,34,35]. Apart from these downsides, as composite bars show brittleness and linear behavior in tensile tests, they do not provide an advance warning before failure [33]. Therefore, the hybridization process was proposed to deal with composite bars' problems. Since in this approach, materials with different ultimate tensile strains fail on different levels, hybrid composite bars show pseudo-ductile behavior.

Guowei et al. [35] made hybrid bars from steel and basalt fibers. The steel material was placed in the center of the bars as a core, and the basalt fibers were placed around them as a coating. Their test results show an increase in the ductility of the samples. In addition, this method showed a 169% increase in the modulus of elasticity of this type of hybrid bars compared to composite bars made of glass fibers. YH Cui et al. [36] made only one type of composite hybrid bar using carbon, Twaron, glass, and steel fibers. They showed that the bar was much more resistant to corrosion compared to steel bars, and the modulus of elasticity of 142.11 GPa, which is 71% higher than that of steel bars, has a tensile strength of 628 MPa, which is 156% higher than that of steel bars and also showed proper ductility. Two types of hybrid composite bars were fabricated by Y Liang et al. [37]. In the first type, carbon fibers were placed in the core of the bar with glass fibers around it, and in the other type, carbon fibers were distributed irregularly in the cross-section of the bars. These samples were evaluated under a tensile test. The results of the stress test show a yield limit of 1153 MPa and a final stress of 1191 MPa with a final strain of 3.5%. DW Seo [38] evaluated the effect of the hybrid process on the modulus of elasticity of composite bars made of glass fibers. Two types of composite hybrid bars were fabricated and evaluated. The first type, steel bars, were spread in the core, and the second type, steel wires, were spread in the sample section; glass fibers were used as a coating for both samples. The experimental results show that the hybrid process improved the modulus of elasticity of the composite hybrid bars by up to 270% compared to the composite glass bars. JH Hwang [39] evaluated two samples of hybrid bars with diameters of 13 and 16 mm and the percentage of steel wires with diameters of 0.5, 1, and 2 mm with steel ratios of 10, 30, 50, and 70%. The results show an increase in the modulus of elasticity of composite hybrid bars from 20 to 190% compared to glass composite bars. L Correia et al. [40] used the braidtrusion process to fabricate two samples of glass–steel and basalt–steel composite hybrid bars and compared the results with glass composite bars. The results of the samples show that this process caused nonlinear behavior in these types of composite hybrid bars. Sun et al. [41] investigated steel–FRP composite bars under tensile and compressive loads. Their results show that the failure of these bars under compressive loads can be divided into three categories, including no buckling, post-yield buckling, and elastic buckling. Mirdarsoltany et al. [29] investigated the effect of the hybridization process on the mechanical behavior of glass-fiber-reinforced-polymer (GFRP) bars. The results showed that this process could improve the elastic modulus and ductility of the GFRP bars. Tang et al. [42] investigated the behavior of hybrid composite bars under compression. Their results show that compressive yield load of hybrid composite bars had nothing to do with the slender ratios, and the ultimate compressive load was inversely relevant to the slender ratio. Sun et al. [41] carried out research to evaluate the tensile and compressive behavior of hybrid composite bars. Their results indicate that there are three different modes of failure under compressive loads, including elastic buckling, post-yield buckling, and no buckling.

In this research project, four types of sustainable basalt-fiber-reinforced-polymer (BFRP) hybrid composite bars were developed with carbon T300, steel bar, and steel wire, and then their mechanical behavior and their modes of failure were investigated under tension.

With all the downsides of composite bars discussed, the hybridization process was used to enhance the ductility of BFRP composite bars. This method prevents sudden collapse and provides warning signs before structural failure in concrete elements reinforced with hybrid composite bars. In this research, a novel cross-sectional area for hybrid composite bars was proposed, including steel wires and basalt fibers for fabricating them. Furthermore, the effect of the number of fibers was also evaluated by fabricating a group of hybrid composite bars with different numbers of fibers but with the same proportion of steel to basalt fibers. The proposed cross-sectional area for hybrid composite bars showed more appropriate mechanical behavior in comparison with other types of hybrid composite bars in terms of tensile strength and energy absorbed in the tensile test. Furthermore, as many studies mainly focused on the effects of the hybridization process on the mechanical behavior of GFRP bars and only a limited number of studies investigated the influence of this process on BFRP bars, the main aim of this study was to fabricate and evaluate different types of hybrid composite bars using basalt fibers. The weight of this new hybrid composite bar is lighter than the steel bar, which can lead to a decreased overall weight of RC elements.

2. Materials and Methods

In the present study, the effect of the hybrid process on reducing the weaknesses of composite bars using different fibers was investigated. In making these samples, carbon fibers, basalt fibers, steel bars with a diameter of 6 mm, and steel wires with a thickness of 1.5 mm were used. A total of 12 composite hybrid bars with a length of 450 mm and a diameter of 10 mm were fabricated in 4 groups. Group A consisted of 3 composite hybrid bars with 6 mm steel bars in their core and basalt composite fibers as a coating. In this group, 36% of the cross-sectional area is made of steel, and 64% is composed of basalt roving composite fibers. Group B consisted of 3 hybrid composite bars with steel wires in the core and basalt composite fibers used as cover. In this section, 22% of the cross-sectional area was made of steel wires, and 78% was composed of basalt composite fibers. Group C was similar to Group B in terms of total cross-section of basalt fibers; however, to evaluate the effect of the number of fibers for fabricating hybrid composite bars, the number of composite fibers used in Group C was higher than that used in Group B. Group D consisted of 3 hybrid composite bars made of carbon fiber and basalt composite fibers. The carbon fiber was used in the core of the bars, and basalt fiber was used as the core coating. This type of composite hybrid bar is composed of 30% of the surface area of carbon roving fibers and 70% of basalt fibers. The mechanical properties of the materials used in the fabrication of these bars are shown in Table 1. In addition, in Figure 1, the cross-sections of these bars are shown. The test results were compared with GFRP bars [23]. Furthermore, the modulus of elasticity of composite hybrid bars was compared with the modulus of elasticity obtained from theoretical relationships.

Table 1. Properties of materials used in fabricating hybrid composite bars.

Materials	Tensile Strength (MPa)	Elastic Modulus (GPa)	Tensile Elongation (%)
Carbon T300 fibers	1230–1540	225	1.25–1.5
Basalt fibers	1050–1100	72	2.8–3
Steel wires	1270–1470	200	20
Steel bar	400	200	20
Vinyl ester 901	75	3	4.5–5

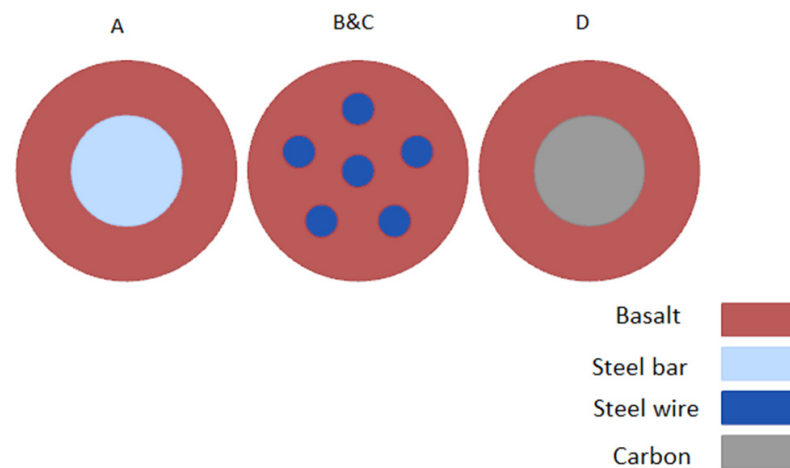


Figure 1. Cross-section of composite hybrid bars. (A) hybrid bars fabricated by Carbon and Basalt fiber; (B) and (C) hybrid bars fabricated by Steel wire and Basalt fiber. (D) hybrid bars fabricated by Steel bar and Basalt fiber.

3. Experimental Program

3.1. Fabrication of Hybrid Composite Bars

Hybrid composites are made from a combination of two or more types of fibers. The nature of this method is to make a new material that retains the positive properties of its constituent fibers and eliminates their weaknesses. This process, depending on the type of fibers used, has an essential effect on increasing the modulus of elasticity and ductility of fiber-reinforced-plastic (FRP) bars. In this research, four types of composite hybrid bars were studied in terms of tensile strength, elastic modulus, and energy absorbed. To fabricate these types of bars, a pultrusion device was used with the hybridization process method as shown in Figure 2. This method is used to fabricate fiber-reinforced plastics with a constant cross-section. In this process, the fibers are pulled through a heated die. While passing through the die, a constant pressure is applied, resulting in the resin melting and its impregnation into the fibrous reinforcement [43].



Figure 2. Pultrusion machine used to manufacture composite hybrid bar.

After impregnating the fibers with vinyl ester resin, the materials were fabricated using the mold shown in Figure 3a and regularly fed into the pultrusion device to make these bars. As shown in Figure 3b, to fabricate hybrid composite bars in Groups A, B, and C, steel bars or steel wires were placed in the middle circle of the mold and basalt fibers were situated in the outer-circle rows. As for Group D, carbon fibers were positioned in the inner circle row, and basalt fibers were situated in the outer one.

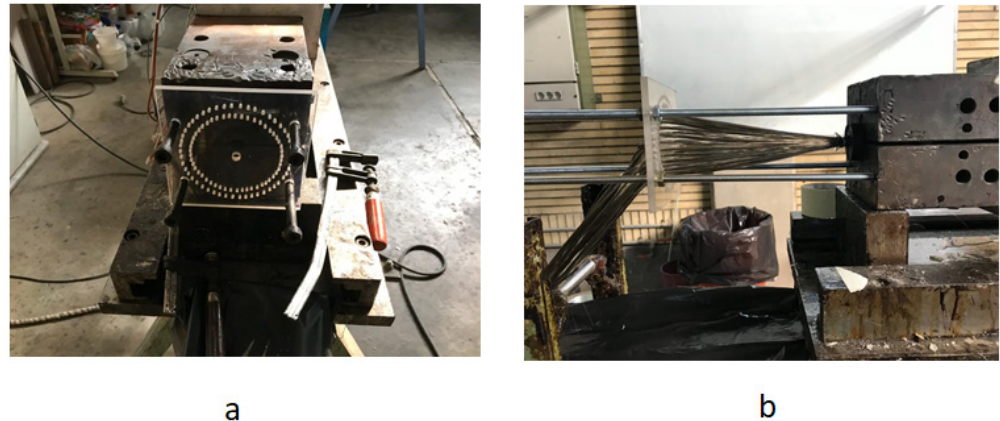


Figure 3. (a) The mold made to enter the fibers of the pultrusion machine; (b) the way of fibers entering the pultrusion device.

3.2. Specimen Preparation for Tensile Test

In order to perform the tensile test on the manufactured specimens, the composite bar with 10 mm in diameter, which is a common diameter in the industry [44], was placed inside a steel tube (grips) at 120 mm on both ends. The steel grip had an outer diameter of 14 mm and a thickness of 4 mm. The gap between the steel tube and the hybrid composite bar was filled with a special adhesive to ensure that the specimens did not slip during the tensile test. Figure 4 shows how to prepare the bars for the tensile test.

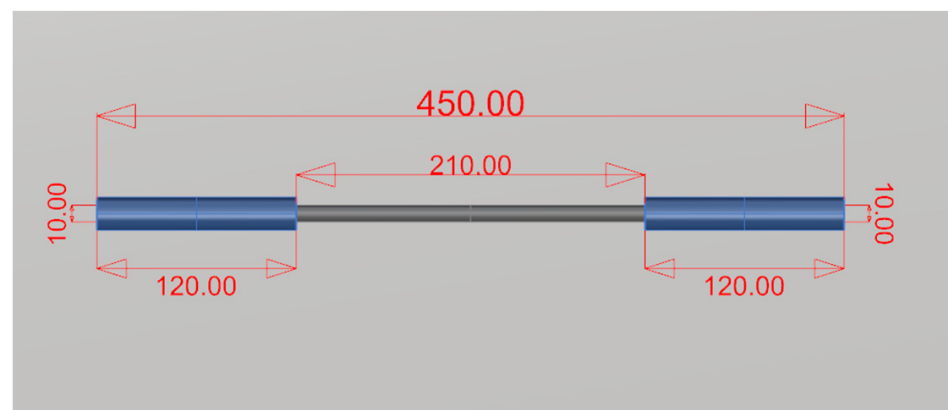


Figure 4. Specimen layout for tensile test.

ACI 440K [44] standard was used in order to investigate the tensile behavior of the manufactured bars. A shank machine was used to perform tensile testing in these specimens. After preparing the samples and the hybrid composite bars, they were placed in the grip of the shank machine as shown in Figure 5. The device then applied traction to the samples at a speed of 0.5 mm/s.



Figure 5. Shank machine for applying tensile test.

4. Results and Discussion

4.1. Theoretical Calculation

In general, the modulus of elasticity of E_H hybrid composites is obtained directly from the following formula [45]:

$$E_H = \sum_{i=1}^n E_i V_i, \quad (1)$$

where E_i and V_i are the module and volume of number i of the fiber that was used to fabricate hybrid composite bars. To make the calculations easier, the properties of the resin in this formula can be omitted.

Tensile strength and modulus of elasticity are obtained using the data obtained from the tensile test in accordance with Equations (2) and (3) which are provided according to the CSA standard [46].

$$f_u = \frac{P_{Max}}{A_{Rebar}}, \quad (2)$$

In which, f_u is the tensile strength (Pa), P_{max} is the maximum tensile force (N) and A_{Rebar} is the cross-sectional area of the rebar (m^2).

According to the CSA standard [45], the modulus of elasticity of a composite rebar is obtained from Equation (3).

$$E_{Hybrid} = \frac{(P_1 - P_2)}{(\varepsilon_1 - \varepsilon_2) A_{Rebar}}, \quad (3)$$

In this formula, E_{Hybrid} is the modulus of elasticity of the hybrid rebar (Pa). P_1 and P_2 are the forces corresponding to 50% and 25% of the maximum force applied in the tensile test (N). ε_1 and ε_2 are the corresponding strains for these forces P_1 and P_2 . A_{Rebar} is the cross-sectional area of the rebar (m^2).

Table 2 shows different hybrid composite bars fabricated as well as the modulus of elasticity of the theory obtained from Equation (1).

Table 2. Characteristics of four types of hybrid composite bars.

Bar Types	Diameter (mm)	Steel Cross-Section Area	Basalt Cross-Section Area	Carbon Cross-Section Area	Theoretical EH (GPa)
A	10	36%	64%	0	102
B	10	22%	78%	0	74
C	10	22%	78%	0	55
D	10	0%	70%	30%	114

4.2. Theoretical Calculation

4.2.1. Tensile Strength and Elastic Modulus

Table 3 shows the mean values of tensile strength as well as the modulus of elasticity obtained from the experimental tests. The results represent the average values of three tests for each group type. The results of this section were compared with the values of the modulus of elasticity obtained from Equation (1).

Table 3. Comparison of the modulus of elasticity of hybrid bars between experiments and Equation (1).

Types of Composite Hybrid Bar	Tensile Strength (MPa)	Experimental Elastic Modulus (GPa)	Theoretical Elastic Modulus (GPa)
A	798.6	88	102
B	917.4	63	74
C	1027.3	55	55
D	869.7	106	110

As can be seen from Table 3, the modulus of elasticity obtained from Equation (1) is a good estimate of laboratory values. Figure 6 shows the experimental and theoretical elastic modulus of three types of hybrid composite bars. There is an almost 15% difference in the elastic modulus for Groups A and B between the theoretical and experimental values, and this can be attributed to the higher amount of the resin used for their fabrication and omitting this amount to make the calculation easier.

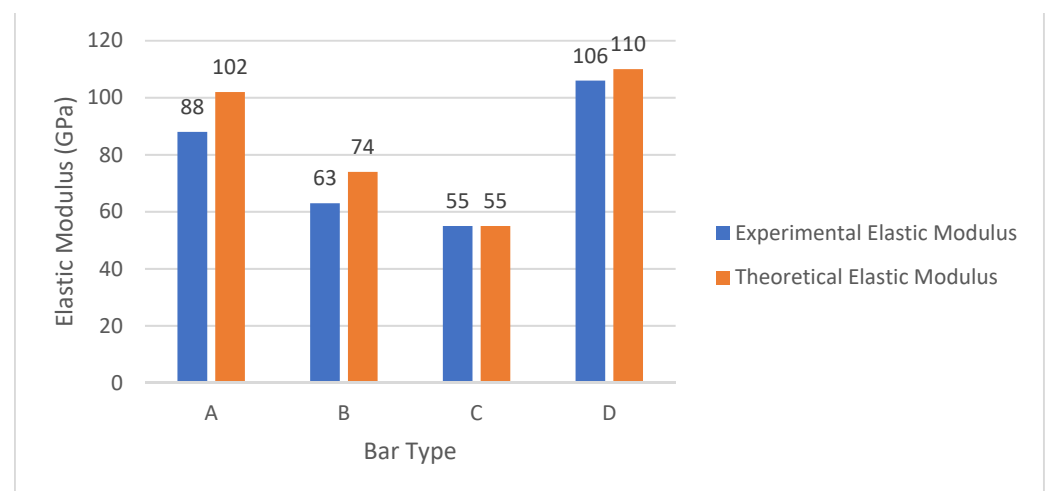


Figure 6. Tensile elastic modulus for the hybrid composite bars.

Figure 7 shows the strain–stress diagrams of hybrid composite bars obtained from laboratory results for the four groups. As can be seen, the diagram of these samples does not show linear behavior until rupture and has a pseudo-ductile behavior that is the result of using a hybrid process in the fabrication of this type of bars.

According to Figure 7b,c, for the same cross-section area of hybrid composite bars, improving the number of fibers can lead to an increased ultimate tensile strength of these bars. This is due to the high tensile strength of these composite fibers; the more fibers are used, the higher tensile strength composite hybrid bars have. However, by increasing fibers in hybrid composite bars' cross-section, their elastic modulus decreases. Figure 8 demonstrates the mean value of tensile tests' results until their ultimate tensile strength for all types of composite hybrid bars.

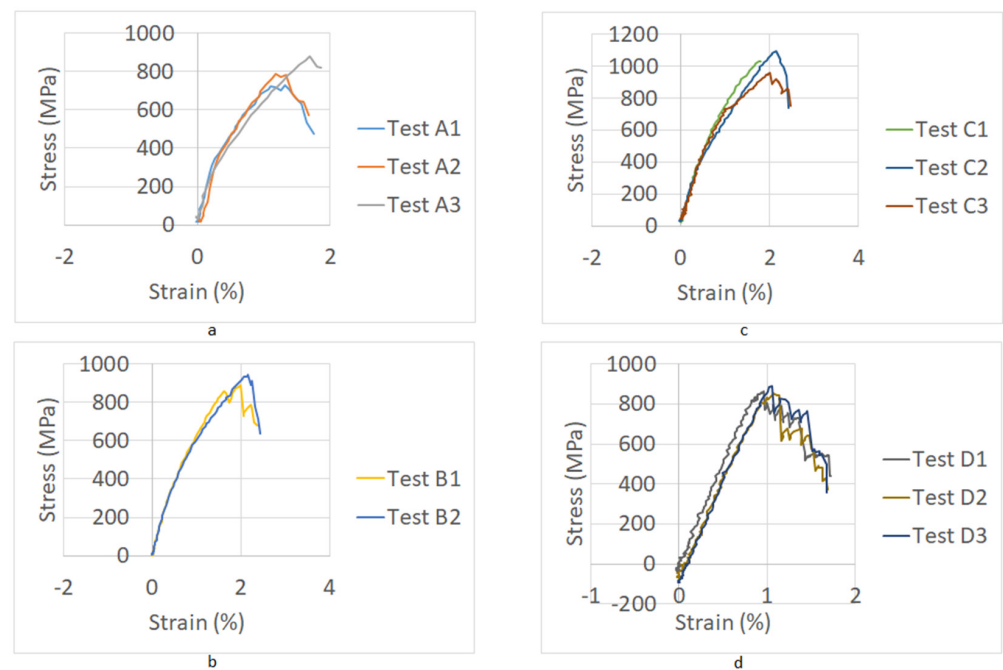


Figure 7. Tensile results of hybrid composite bars: (a) type A, (b) type B, (c) type C, (d) type D.

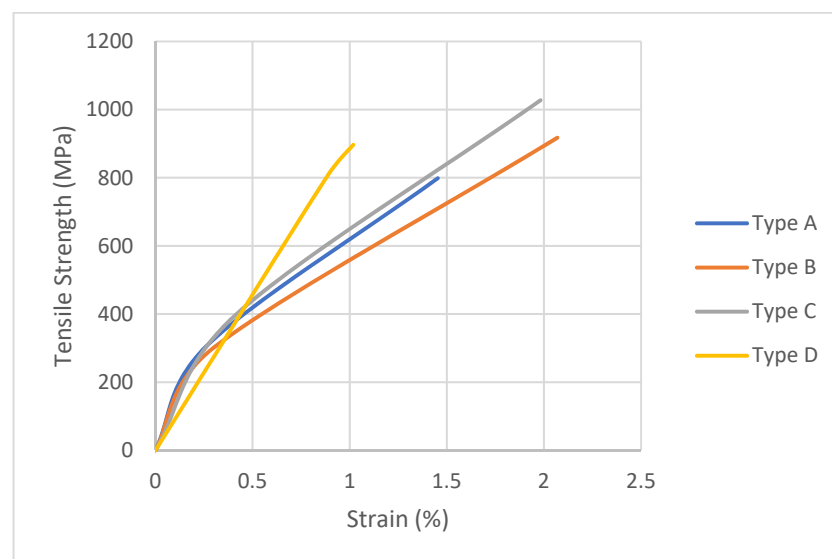


Figure 8. Mean value for tensile tests' results of all four types of hybrid composite bars.

Figure 9 shows the tensile ultimate strength and tensile yield strength of the four types of hybrid composite bars.

Table 4 shows that, generally, the hybridization process can lead to an improved elastic modulus and tensile strength of composite bars in comparison with GFRP bars [44].

Table 4. Comparison of the modulus of elasticity and tensile strength of hybrid composite bars with GFRP bars [44].

Types of Composite Hybrid Bar	Tensile Strength (MPa)	Experimental Elastic Modulus (GPa)	Improvement in Elastic Modulus (%)	Improvements in Tensile Strength (%)
A	798.6	88	83.3	−2.03
B	917.4	63	31.25	12.53
C	1027.3	55	14.58	26.01
D	869.7	106	120.83	6.68
GFRP	815.23	48	—	—

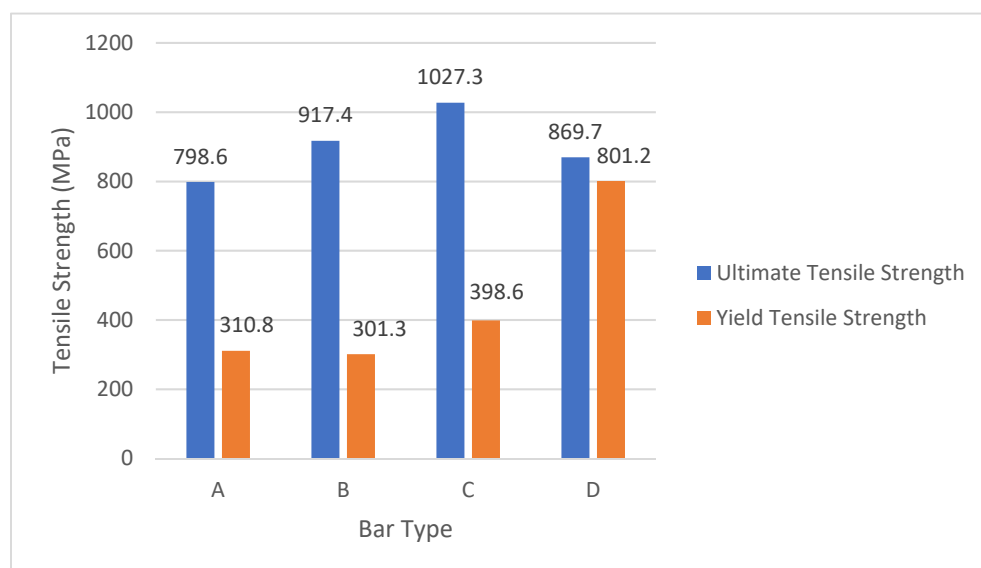


Figure 9. Tensile strength test results for the hybrid composite bars.

4.2.2. Mode of Rapture in Tensile Test

Figures 10–13 demonstrate failure characteristics of hybrid composite bars.



Figure 10. Failure characteristics of a hybrid composite bar type A.



Figure 11. Failure characteristics of a hybrid composite bar type B.



Figure 12. Failure characteristics of a hybrid composite bar type C.



Figure 13. Failure characteristics of a hybrid composite bar type D.

According to tensile tests, in type A hybrid composite bars, in the first stage, steel bars reached their ultimate strength, and finally basalt fibers fractured.

According to tensile tests, in Groups B and C, in the first stage, steel wires reached their ultimate strength, and after that basalt fibers fractured.

According to tensile tests, in type D manufactured bars, in the first stage, carbon fibers reached their ultimate strength, and finally basalt fibers fractured. Tensile tests showed that, in all types of hybrid composite bars, failure modes were identical. Indeed, at first materials with a higher elastic modulus fail, and then materials with a lower elastic modulus reach their ultimate strength and fail.

4.3. Comparison of Hybrid Composite Bars' Absorbed Energy

To calculate the amount of energy absorbed in hybrid composite bar specimens, the area under the force and displacement diagram of each bar was calculated, which is shown in Table 5. The area below this diagram is equal to Equation (4).

$$\int_0^{du} F \cdot dl, \quad (4)$$

Table 5. Energy absorbed by four types of hybrid composite bars.

Types of Composite Hybrid Bar	Mean Value for Energy Absorbed (J)
A	30.45
B	62.33
C	72.03
D	25.97

In this equation, du is the final rise of the section, dl is the differential rise, and F is the ram force.

According to Table 5, specimens in Group C have the highest amount of energy absorbed in comparison with other specimens. This could be due to the presence of the steel wires in the cross-sectional area of these bars. However, Group D specimens show the least energy absorbed. This result could be attributed to using brittle materials, including basalt and carbon fibers in their fabrication.

5. Conclusions

One of the main problems of steel bars in reinforced-concrete elements is the corrosion of this type of bars. In this study, four types of BFRP hybrid composite bars were manufactured to provide a feasible and practical alternative to RC elements in a corrosive environment. In addition, they are more durable in comparison with steel bars, and this is the reason for using such bars as sustainable materials for construction. This process protects the surface of the steel bars and wires from corrosion. In addition, such hybridization improves the ductility of BFRP bars, leads to pseudo-ductile behavior, and provides the feasibility of their usage in concrete elements because of their low-cost and light-weight characteristics.

The hybrid process can optimally provide acceptable tensile strength and modulus of elasticity properties. The results show that this process increases the modulus of elasticity of hybrid composite bars up to 120% compared to GFRP composite bars and also increases the tensile strength of these bars up to 206% compared to steel bars ST37.

Furthermore, although this study shows the potential application of using the proposed BFRP hybrid composite bar as reinforcement for concrete elements, more investigation should be carried out to investigate their long-term performance under different environmental conditions, their performance under cyclic loads, their behavior under compressive load, and their other mechanical properties.

Author Contributions: Conceptualization, M.M.; methodology, M.M.; software, M.M.; validation, M.M., F.H. and A.R.; formal analysis, M.M.; investigation, M.M.; resources, M.M.; writing—original draft preparation, M.M. and R.H.; writing—review and editing, F.A. and R.H.; supervision, A.R.; project administration, M.M.; funding acquisition, M.M. All authors have read and agreed to the published version of the manuscript.

Funding: This research received no external funding.

Institutional Review Board Statement: Not applicable.

Informed Consent Statement: Not applicable.

Data Availability Statement: Data can be accessed by contacting the following email address: Amin.st@aut.ac.ir.

Acknowledgments: Special thanks to Dorsa Ghodsian and Mohammad Sanei for their tremendous help in this research.

Conflicts of Interest: The authors declare no conflict of interest.

References

1. Du, J.; Wang, C.; Qiao, M.; Chang, X.; Chen, H. Flexural behavior of concrete beams reinforced by CFRP bars. In Proceedings of the 2010 International Conference on Mechanic Automation and Control Engineering, Wuhan, China, 26–28 August 2010; pp. 1060–1063. [\[CrossRef\]](#)
2. Tawfik, T.A.; Metwally, K.A.; El-Beshlawy, S.A.; Al Saffar, D.M.; Tayeh, B.A.; Hassan, H.S. Exploitation of the nanowaste ceramic incorporated with nano silica to improve concrete properties. *J. King. Saud. Univ.-Eng. Sci.* **2020**, in press. [\[CrossRef\]](#)
3. Zeyad, A.M.; Khan, A.H.; Tayeh, B.A. Durability and strength characteristics of high-strength concrete incorporated with volcanic pumice powder and polypropylene fibers. *J. Mater. Res. Technol.* **2020**, *9*, 806–813. [\[CrossRef\]](#)
4. Agwa, I.S.; Omar, O.M.; Tayeh, B.A.; Abdelsalam, B.A. Effects of using rice straw and cotton stalk ashes on the properties of lightweight self-compacting concrete. *Constr. Build. Mater.* **2020**, *235*, 117541. [\[CrossRef\]](#)
5. Alexander, M.; Beushausen, H. Durability, service life prediction, and modelling for reinforced concrete structures—Review and critique. *Cem. Concr. Res.* **2019**, *122*, 17–29. [\[CrossRef\]](#)
6. Almusallam, T.H.; Elsanadedy, H.M.; Al-Salloum, Y.A.; Alsayed, S.H. Experimental and numerical investigation for the flexural strengthening of RC beams using near-surface mounted steel or GFRP bars. *Constr. Build. Mater.* **2013**, *40*, 145–161. [\[CrossRef\]](#)
7. Kassem, C.; Farghaly, A.S.; Benmokrane, B. Evaluation of flexural behavior and serviceability performance of concrete beams reinforced with FRP bars. *J. Compos. Constr.* **2011**, *15*, 682–695. [\[CrossRef\]](#)
8. Kazemian, M.; Sedighi, S.; Ramezani-pour, A.A.; Bahman-Zadeh, F.; Ramezani-pour, A.M. Effects of cyclic carbonation and chloride ingress on durability properties of mortars containing Trass and Pumice natural pozzolans. *Struct. Concr.* **2021**, 1–16. [\[CrossRef\]](#)
9. Valipour, M.; Pargar, F.; Shekarchi, M.; Khani, S.; Moradian, M. In situ study of chloride ingress in concretes containing natural zeolite, metakaolin and silica fume exposed to various exposure conditions in a harsh marine environment. *Constr. Build. Mater.* **2013**, *46*, 63–70. [\[CrossRef\]](#)
10. Liang, M.-T.; Huang, R.; Jheng, H.-Y. Reconsideration for a study of the effect of chloride binding on service life predictions. *J. Mar. Sci. Technol.* **2011**, *19*, 531–540. [\[CrossRef\]](#)
11. Skrzypkowski, K. An experimental investigation into the stress-strain characteristic under static and quasi-static loading for partially embedded rock bolts. *Energies* **2021**, *14*, 1483. [\[CrossRef\]](#)
12. Abed, F.; Mehaini, Z.; Oucif, C.; Abdul-Latif, A.; Baleh, R. Quasi-static and dynamic response of GFRP and BFRP bars under compression. *Compos. Part C Open Access* **2020**, *2*, 100034. [\[CrossRef\]](#)
13. Al-Rahmani, A.; Abed, F.H. Numerical investigation of hybrid FRP reinforced beams. In Proceedings of the 2013 5th International Conference on Modeling, Simulation and Applied Optimization (ICMSAO), Hammamet, Tunisia, 28–30 April 2013. [\[CrossRef\]](#)
14. Sun, Z.Y.; Yang, Y.; Qin, W.H.; Ren, S.T.; Wu, G. Experimental study on flexural behavior of concrete beams reinforced by steel-fiber reinforced polymer composite bars. *J. Reinf. Plast. Compos.* **2012**, *31*, 1737–1745. [\[CrossRef\]](#)
15. El Refai, A.; Abed, F.; Al-Rahmani, A. Structural performance and serviceability of concrete beams reinforced with hybrid (GFRP and steel) bars. *Constr. Build. Mater.* **2015**, *96*, 518–529. [\[CrossRef\]](#)
16. Homayoonmehr, R.; Ramezani-pour, A.A.; Mirdarsoltany, M. Influence of metakaolin on fresh properties, mechanical properties and corrosion resistance of concrete and its sustainability issues: A review. *J. Build. Eng.* **2021**, *44*, 103011. [\[CrossRef\]](#)
17. Mirdarsoltany, M.; Rahai, A.; Kabir, M.Z. Performance Evaluation of CFRP Strengthened Corrosion-Proof Columns. *Shock Vib.* **2021**, *2021*, 8390088. [\[CrossRef\]](#)
18. Safehian, M.; Ramezani-pour, A.A. Assessment of service life models for determination of chloride penetration into silica fume concrete in the severe marine environmental condition. *Constr. Build. Mater.* **2013**, *48*, 287–294. [\[CrossRef\]](#)
19. Valipour, M.; Pargar, F.; Shekarchi, M.; Khani, S. Comparing a natural pozzolan, zeolite, to metakaolin and silica fume in terms of their effect on the durability characteristics of concrete: A laboratory study. *Constr. Build. Mater.* **2013**, *41*, 879–888. [\[CrossRef\]](#)
20. Ramezani-pour, A.A.; Riahi Dehkordi, E.; Ramezani-pour, A.M. Influence of Sulfate Ions on Chloride Attack in Concrete Mortars Containing Silica Fume and Jajrood Trass. *Iran J. Sci. Technol. Trans. Civ. Eng.* **2020**, *44*, 1135–1144. [\[CrossRef\]](#)
21. Zolfagharnasab, A.; Ramezani-pour, A.A.; Bahman-zadeh, F. Investigating the potential of low-grade calcined clays to produce durable LC 3 binders against chloride ions attack. *Constr. Build. Mater.* **2021**, *303*, 124541. [\[CrossRef\]](#)
22. Vedalakshmi, R.; Rajagopal, K.; Palaniswamy, N. Longterm corrosion performance of rebar embedded in blended cement concrete under macro cell corrosion condition. *Constr. Build. Mater.* **2008**, *22*, 186–199. [\[CrossRef\]](#)
23. Flores Medina, N.; Barluenga, G.; Hernández-Olivares, F. Combined effect of Polypropylene fibers and Silica Fume to improve the durability of concrete with natural Pozzolans blended cement. *Constr. Build. Mater.* **2015**, *96*, 556–566. [\[CrossRef\]](#)
24. Elgabbas, F.; Ahmed, E.A.; Benmokrane, B. Physical and mechanical characteristics of new basalt-FRP bars for reinforcing concrete structures. *Constr. Build. Mater.* **2015**, *95*, 623–635. [\[CrossRef\]](#)
25. Elgabbas, F.; Ahmed, E.A.; Benmokrane, B. Flexural Behavior of Concrete Beams Reinforced with Ribbed Basalt-FRP Bars under Static Loads. *J. Compos. Constr.* **2017**, *21*, 04016098. [\[CrossRef\]](#)

26. Barris, C.; Torres, L.; Turon, A.; Baena, M.; Catalan, A. An experimental study of the flexural behaviour of GFRP RC beams and comparison with prediction models. *Compos. Struct.* **2009**, *91*, 286–295. [[CrossRef](#)]
27. Ferreira, A.J.M.; Camanho, P.P.; Marques, A.T.; Fernandes, A.A. Modelling of concrete beams reinforced with FRP re-bars. *Compos. Struct.* **2001**, *53*, 107–116. [[CrossRef](#)]
28. Mirdarsoltany, M.; Rahai, A.; Hatami, F. Experimental Investigation on the Ductility of Concrete Deep Beams Reinforced with Basalt-Carbon and Basalt-Steel Wire Hybrid Composite Bars. *Shock Vib.* **2021**, *2021*, 6866993. [[CrossRef](#)]
29. Mirdarsoltany, M.; Rahai, A.; Hatami, F. Tensile behavior of GFRP hybrid composite bars in RC structures. *Solid State Technol.* **2021**, *64*, 4955–4961.
30. Saleh, Z.; Sheikh, M.N.; Remennikov, A.M.; Basu, A. Numerical investigations on the flexural behavior of GFRP-RC beams under monotonic loads. *Structures* **2019**, *20*, 255–267. [[CrossRef](#)]
31. Shin, S.; Seo, D.; Han, B. Performance of concrete beams reinforced with GFRP bars. *J. Asian Archit. Build. Eng.* **2009**, *8*, 197–204. [[CrossRef](#)]
32. Wang, H.; Belarbi, A. Ductility characteristics of fiber-reinforced-concrete beams reinforced with FRP rebars. *Constr. Build. Mater.* **2011**, *25*, 2391–2401. [[CrossRef](#)]
33. Elgabbas, F.; Vincent, P.; Ahmed, E.A.; Benmokrane, B. Experimental testing of basalt-fiber-reinforced polymer bars in concrete beams. *Compos. Part B Eng.* **2016**, *91*, 205–218. [[CrossRef](#)]
34. Castro, P.F.; Carino, N.J. Tensile and nondestructive testing of FRP bars. *J. Compos. Constr.* **1998**, *2*, 17–26. [[CrossRef](#)]
35. Ma, G.; Huang, Y.; Aslani, F.; Kim, T. Tensile and bonding behaviours of hybridized BFRP-steel bars as concrete reinforcement. *Constr. Build. Mater.* **2019**, *201*, 62–71. [[CrossRef](#)]
36. Cui, Y.H.; Tao, J. A new type of ductile composite reinforcing bar with high tensile elastic modulus for use in reinforced concrete structures. *Can. J. Civ. Eng.* **2009**, *36*, 672–675. [[CrossRef](#)]
37. Liang, Y.; Sun, C.; Ansari, F. Acoustic Emission Characterization of Damage in Hybrid Fiber-Reinforced Polymer Rods. *J. Compos. Constr.* **2004**, *8*, 70–78. [[CrossRef](#)]
38. Seo, D.-W.; Park, K.-T.; You, Y.-J.; Kim, H.-Y. Enhancement in Elastic Modulus of GFRP Bars by Material Hybridization. *Engineering* **2013**, *5*, 865–869. [[CrossRef](#)]
39. Hwang, J.-H.; Seo, D.-W.; Park, K.-T.; You, Y.-J. Experimental Study on the Mechanical Properties of FRP Bars by Hybridizing with Steel Wires. *Engineering* **2014**, *6*, 365–373. [[CrossRef](#)]
40. Correia, L.; Cunha, F.; Mota, C.; Figueiro, R.; Nunes, J.P. Pseudo-ductile Braided Composite Rods (BCRs) produced by Braidtrusion. In Proceedings of the 17th European Conference on Composite Materials (ECCM), Munich, Germany, 26–30 June 2016; pp. 26–30.
41. Sun, Z.; Tang, Y.; Luo, Y.; Wu, G.; He, X. Mechanical Properties of Steel-FRP Composite Bars under Tensile and Compressive Loading. *Int. J. Polym. Sci.* **2017**, *2017*, 5691278. [[CrossRef](#)]
42. Tang, Y.; Sun, Z.; Wu, G. Compressive behavior of sustainable steel-FRP composite bars with different slenderness ratios. *Sustainability* **2019**, *11*, 1118. [[CrossRef](#)]
43. Sandberg, M.; Yuksel, O.; Comminal, R.B.; Sonne, M.R.; Jabbari, M.; Larsen, M.; Hattel, J.H.; Salling, F.B.; Baran, I.; Spangenberg, J. Numerical modeling of the mechanics of pultrusion. In *Mechanics of Materials in Modern Manufacturing Methods and Processing Techniques*; Elsevier: Amsterdam, The Netherlands, 2020; pp. 173–195. [[CrossRef](#)]
44. ACI Committee 440.1R-06. *Guide for the Design and Construction of Concrete Reinforced with FRP Bars*; American Concrete Institute: Farmington Hills, MI, USA, 2006; p. 44.
45. Szmigiera, E.D.; Protchenko, K.; Urba Ski, M.; Garbacz, A. Mechanical properties of hybrid FRP bars and nano-hybrid FRP bars. *Arch. Civ. Eng.* **2019**, *65*, 97–110. [[CrossRef](#)]
46. Canadial Standards Association. *Design and Construction of Building Structures with Fibre-Reinforced Polymers*; S806-12 CAN/CSA: Mississauga, ON, Canada, 2012.